Study of the pygmy dipole resonance in the interacting boson approximation framework

S. Pascu,[1,2] J. Endres,[1] N. V. Zamfir,[2] and A. Zilges[1]
[1]*Institut für Kernphysik, Universität zu Köln, Zülpicher Strasse 77, D-50937 Köln, Germany*
[2]*National Institute for Physics and Nuclear Engineering, R-77125, Bucharest-Magurele, Romania*
(Received 13 February 2012; revised manuscript received 24 May 2012; published 14 June 2012)

Background: The pygmy dipole resonance (PDR) is an interesting nuclear structure phenomenon with an impact in predicting different astrophysics scenarios, for example, specific properties of neutron stars that can be determined from the thickness of the neutron skin which is directly connected to the strength of the PDR. Various collective and microscopic models were employed in order to account for the observed properties of the PDR.
Purpose: Determine for the first time whether it is possible to use the interacting boson approximation (IBA) to reproduce the general characteristics of the PDR.
Methods: The PDR properties of the stable even-even $N = 82$ isotones are calculated in the IBA-$spdf$ model based on the assumption that many effects of the mixing caused by the shell structure can be simulated by considering the number of bosons as an effective value.
Results: The IBA calculations indicate a resonance-like structure of the $E1$ strength in the energy region 5–8 MeV, thus confirming the experimental results for this mass region. The distribution and fragmentation of the $J^\pi = 1^-$ states and of the $E1$ strength are in good agreement with the experimental data. By employing the same procedure as for the $N = 82$ isotones, the model is used to predict the PDR strength for a nucleus in a different mass region, i.e., for the ^{94}Mo nucleus.
Conclusions: The calculations confirm a good agreement for the distribution and fragmentation of the $E1$ strength.

DOI: 10.1103/PhysRevC.85.064315 PACS number(s): 21.10.Re, 21.60.Fw, 24.30.Cz

I. INTRODUCTION

In the last few decades many experimental and theoretical investigations have been devoted to the study of electric dipole excitations in atomic nuclei. It has been found that in addition to the well-established isovector electric giant dipole resonance (IVGDR) [1] another concentration of dipole strength is observed at excitation energies around the neutron-separation energy. This bunching of strong dipole transitions has been named pygmy dipole resonance (PDR) and has attracted considerable interest during the last few years [2–12]. Various high-resolution experiments have revealed details of the strength distribution of this excitation mode in different mass regions of the nuclear chart. Furthermore, it was predicted that the strength of the PDR is related to the oscillation of the neutron skin against a symmetric proton-neutron core [13,14]. To confirm this picture the $E1$ response of nuclei far from the β-stability line has to be measured, which will allow the extension of the systematics to the very neutron-rich nuclei [15]. Presently, the measurements of the PDR have been restricted mostly to stable nuclei (except, for example, the experiments on ^{130,132}Sn [5] and ^{68}Ni [8]). The observed concentration of collective strength close to the particle threshold is not only an interesting nuclear structure phenomenon but also has an important impact in predictions of neutron capture rates in the r-process nucleosynthesis [16,17]. Also the thickness of the neutron skin, which can be determined from the strength of the PDR, can be connected to different properties of neutron stars [18–20].

Various, sometimes contradictory, model descriptions exist to account for the origin of the $E1$ strength. In hydrodynamic and collective approaches, it has been suggested that an oscillation of the neutron-rich nuclear matter at the nuclear skin relative to the rest of the nucleus is responsible for the generation of pygmy resonances [21,22]. Further microscopic calculations, such as density functional calculations [23], quasiparticle random-phase approximations [24,25], calculations in the quasiparticle-phonon model [6,26,27], relativistic quasiparticle time blocking approximations [28], and calculations in the extended theory of finite Fermi systems [29–31], have provided a deeper understanding of this excitation mechanism. The systematics have been extended to the neutron-rich nuclei, indicating a strong correlation between the neutron excess and the observed total $E1$ strength of the PDR.

An important role in nuclear structure is played by the interaction between valence neutrons and protons. This interaction accounts for the onset of deformation, subshell structure, and intruder states in the medium mass region. The structure of nuclei situated very close to a subshell or shell closure is known to be difficult to describe by collective models like the interacting boson approximation (IBA). However, various methods have been applied previously in order to overcome this difficult point. A possible way to do this is within the IBA-2 model (which takes into account separately the proton and neutron degrees of freedom) [32] by mixing two boson configurations differing by two bosons. This procedure has been applied with success to account for the low-lying properties of Mo isotopes [32], Cd [33,34], and Hg [35]. The other approach is provided by the calculations performed in the IBA-1 framework by introducing into the model an effective boson number. This procedure was shown to give similar results as the IBA-2 calculations for Mo and Cd nuclei [36].

In the present paper we report on a description of PDR properties of the stable even-even $N = 82$ isotones in the

IBA-$spdf$ model based on the assumption that many effects of the mixing caused by the shell closure can be simulated by considering the number of bosons as an effective value. The calculations are concentrated on reproducing the main features of the PDR excitations. It is shown that a simple phenomenological model can provide a good description of the number of 1^- states and of the $E1$ decay probabilities of these levels. Furthermore, the distribution and fragmentation of these states is found to be in a good agreement with the experimental values. In the last section of the paper, we use the same procedure to predict the PDR strength in the nonmagic nucleus ^{94}Mo.

The results show a great similarity with the calculations provided by the more modern microscopic models [11]. This confirms the collective nature of the PDR and points to an underlying microscopic structure of the collective behavior taken into account in the IBA calculations.

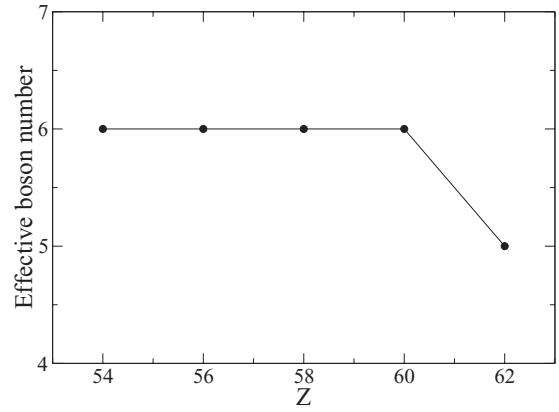

FIG. 1. Effective boson number employed in the present calculations to reproduce the PDR properties of stable even-even $N = 82$ isotones.

II. THEORETICAL FRAMEWORK

The interacting boson model provides a phenomenological approach for studying nuclear structure. In this picture the collective levels in even-even nuclei are constructed as states of a system of N interacting bosons of a given spin. The quadrupole vibration and deformation are described in terms of s and d bosons ($L = 0$ and $L = 2$), while negative parity states are described by introducing p and f bosons ($L = 1$ and $L = 3$).

Calculations were performed in the $spdf$ IBA-1 framework (no distinction is made between protons and neutrons) using the extended consistent Q formalism (ECQF) [37]. The most commonly used form of the IBA-1 Hamiltonian, which allows a clear interpretation of the role provided by each term in determining the structure of the nucleus considered, is the so-called multipole expansion. The Hamiltonian employed in the present paper is the natural extension of the $\hat{H}_{sd}$ Hamiltonian [38]:

$$\hat{H}_{spdf} = \epsilon_d \hat{n}_d + \epsilon_p \hat{n}_p + \epsilon_f \hat{n}_f + \kappa(\hat{Q}_{spdf} \cdot \hat{Q}_{spdf})^{(0)} + a_3[(\tilde{d}^\dagger d)^{(3)} \cdot (\tilde{d}^\dagger d)^{(3)}]^{(0)} + a_4[(\tilde{d}^\dagger d)^{(4)} \cdot (\tilde{d}^\dagger d)^{(4)}]^{(0)}, \quad (1)$$

where ϵ_d, ϵ_p, and ϵ_f are the boson energies and $\hat{n}_p$, $\hat{n}_d$, and $\hat{n}_f$ are the boson number operators. The other two parameters, a_3 and a_4, are introduced to account for the anharmonicities of the nuclei described by the present calculations. In the $spdf$ model [39], the quadrupole operator is given by

$$\hat{Q}_{spdf} = \hat{Q}_{sd} + \hat{Q}_{pf} = \left[(\hat{s}^\dagger \tilde{d} + \hat{d}^\dagger \tilde{s})^{(2)} - \frac{\sqrt{7}}{2}(\tilde{d}^\dagger d)^{(2)}\right] + \frac{3\sqrt{7}}{5}[(p^\dagger \tilde{f} + f^\dagger \tilde{p})]^{(2)} - \frac{9\sqrt{3}}{10}(p^\dagger \tilde{p})^{(2)} - \frac{3\sqrt{42}}{10}(f^\dagger \tilde{f})^{(2)}. \quad (2)$$

This form of the quadrupole operator implies the use of the same quadrupole parameter strength κ to describe both the sd bosons and the pf bosons. In addition, the rotational $SU_{spdf}(3)$ structure is also generated by this form [Eq. (2)] of the $\hat{Q}_{spdf}$ quadrupole operator [39]. In this way, no additional free parameters are used in the calculations.

For the $E1$ transitions there is more than one operator in the $spdf$ algebra. Consequently, a linear combination of the three allowed one-body interactions was taken:

$$\hat{T}(E1) = e_1\left[\chi_{sp}^{(1)}(s^\dagger \tilde{p} + p^\dagger \tilde{s})^{(1)} + (p^\dagger \tilde{d} + d^\dagger \tilde{p})^{(1)} + \chi_{df}^{(1)}(d^\dagger \tilde{f} + f^\dagger \tilde{d})^{(1)}\right], \quad (3)$$

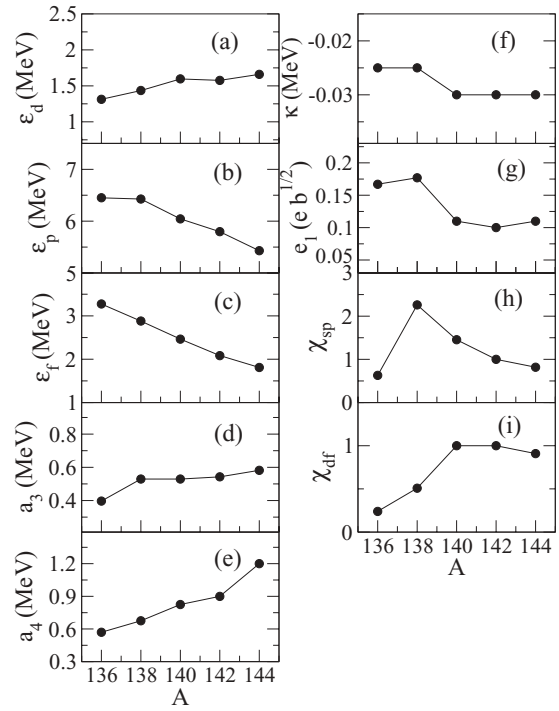

FIG. 2. Evolution of the ϵ_d, ϵ_p, ϵ_f, a_3, a_4, κ, e_1, χ_{sp}, and χ_{df} parameters for the stable even-even $N = 82$ isotones as a function of mass number obtained in the present work. The first six parameters [(a)–(f)] stem from the Hamiltonian of Eq. (1), while the last three [(g)–(i)] belong to the $E1$ transition operator of Eq. (3).

where e_1 is the effective charge for the $E1$ transitions and $\chi_{sp}^{(1)}$ and $\chi_{df}^{(1)}$ are two model parameters.

III. PHENOMENOLOGICAL EFFECTIVE BOSON NUMBER

The number of bosons for a given nucleus is usually equal to half the number of valence particles. However, this definition can become sometimes ambiguous. This is the situation for two different cases. The first case arises when a subshell closure is located inside a major shell. For example, in the $Z = 50$–82 major shell there are strong evidences that $Z = 64$ acts as a subshell closure [40]. The second case arises for nuclei with N or Z close to a magic number. In this situation many states are stemming from two-particle excitations across the shell gap. These effects can be taken into account by the collective models in two ways: (i) by using an IBA-2 description which mixes two different configurations [32] or (ii) by employing an IBA-1 description with a free number of bosons [36] (effective boson number).

By considering the s and d bosons as the shell-model S and D pairs, Scholten [41] proposed a method to calculate the effective boson number in a microscopic model. He proved that for the $Z = 50$–82 shell, the calculations yield a minimum value for $Z = 64$. However, the minimum value is $N_{\rm eff} \simeq 2.4$ instead of 0, what one would expect from the subshell closure. The procedure was applied in Ref. [42] to reproduce the properties of the low-energy levels in Sm isotopes.

In the present calculations it was found that only one set of choice for the effective boson number yielded a better agreement with the experimental values than all other choices. The values employed in the present paper for the effective boson number are presented in Fig. 1. This choice gives a reasonable description of the experimental data, as will be shown below.

IV. RESULTS OF THE IBA-*spdf* CALCULATIONS FOR THE STABLE $N = 82$ ISOTONES

IBA fits were performed for ^{136}Xe, ^{138}Ba, ^{140}Ce, ^{142}Nd, and ^{144}Sm. The calculations were performed with the OCTUPOLE computer code [43]. The Hamiltonian is diagonalized in a Hilbert space with a total number of bosons $N_{\rm eff} = n_s + n_d + n_p + n_f$. For the present calculations we used an extended basis allowing up to three negative parity bosons ($n_p + n_f = 3$). The experimental data are taken from Nuclear Data Sheets [44–48] for the low-lying states and from Refs. [6,11] for the PDR characteristics of the nuclei involved in the present study.

Figure 2 summarizes the IBA parameters employed in the present study, both for the Hamiltonian of Eq. (1) and the $E1$ transition operator from Eq. (3). A free variation of the parameters employed in the Hamiltonian was performed

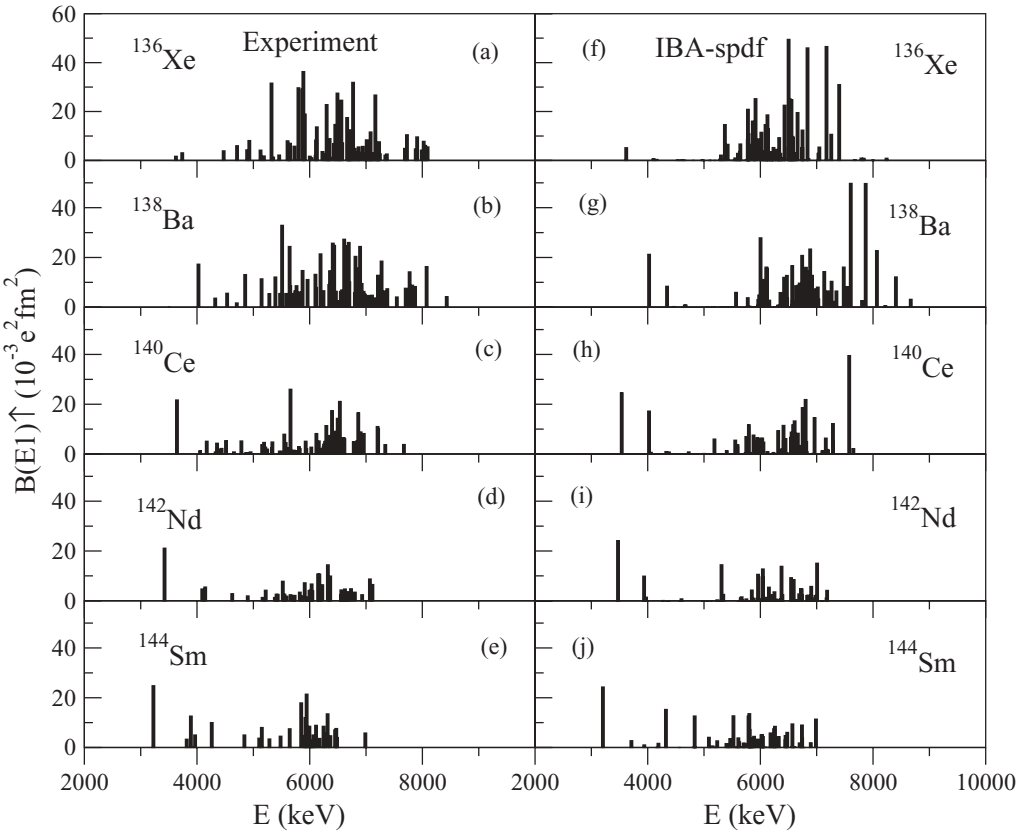

FIG. 3. Comparison between experimental (a)–(e) and calculated (f)–(j) $B(E1)$ strength distributions in stable even-even $N = 82$ isotones. The experimental information concerning the PDR strength is from Refs. [6,11]. IBA calculations give a good reproduction for the strength of these states.

in fact only for κ, a_3, and a_4, while ϵ_d and ϵ_f were fixed at a value corresponding to the energies of the first 2^+ and 3^- states, respectively, of each nucleus. This ensures a good reproduction of the first low-lying levels of the investigated nuclei. In the previous studies of the low-lying states in atomic nuclei [49,50], the energy of the p boson was identified with the energy of the first 1^- state. However, in vibrational nuclei, the first 1^- state arises from the coupling of the first 2^+ and 3^- states. This means that there is no physical justification to include an additional degree of freedom for nuclei situated close to the U(5) symmetry. Therefore, in the present work we identified the p boson with the experimental energy centroid of the $E1$ strength distribution. However, most of the states of the singly magic nuclei do not have a collective character and cannot be reproduced by the IBA calculations. Nevertheless, one has to keep in mind that the PDR is considered as being a collective effect arising from the oscillation of the neutron-rich matter relative to an isospin saturated core of the nucleus. At least such collective effects should be correctly described with a simple collective model. The parameters of the $E1$ transition operator from Eq. (3) were fitted to the absolute $B(E1)$ values in each nucleus.

A comparison between the experimental $B(E1)$ strength distributions and the results of the IBA-$spdf$ calculations for all stable even-even $N = 82$ isotones is shown in Fig. 3. In all cases a resonance-like structure is observed between 5 and 8 MeV in all nuclei, in experiment as well as in calculations. Aside from an energy shift which usually does not exceed 300 keV, there is a good agreement between experiment and theoretical calculations in the shape of the resonance as well as in the increasing strength while increasing the N/Z ratio [although the three parameters in Eq. (3) have no specific dependence on N/Z]. Moreover, the energetic position of the $E1$ strength distribution centroid while going from ^{144}Sm to ^{136}Xe is well reproduced.

TABLE I. Strongest components of the wave functions of the first 1^- state in the stable even-even $N = 82$ nuclei. For illustrative purposes, the representations of the basis states have been simplified and are given in terms of bosons of a specific type: $|[n_s][n_p][n_d][n_f]\rangle$. Only the contributions with an amplitude higher than 10% are included. The components of basis states that are labeled with the same boson numbers are distinguished by other quantum numbers that are not included in this representation.

Nucleus	J_i^π	Main components of the wave function
^{144}Sm	1_1^-	$0.72\|0041\rangle + 0.50\|0041\rangle + 0.43\|1031\rangle$
^{142}Nd	1_1^-	$0.60\|0051\rangle + 0.40\|1041\rangle + 0.40\|1041\rangle + 0.35\|2031\rangle$
^{140}Ce	1_1^-	$-0.44\|2031\rangle - 0.43\|0051\rangle - 0.41\|1041\rangle - 0.40\|1041\rangle$
^{138}Ba	1_1^-	$0.67\|0051\rangle + 0.43\|1041\rangle + 0.32\|1041\rangle + 0.32\|2031\rangle$
^{136}Xe	1_1^-	$-0.61\|4011\rangle + 0.46\|2031\rangle + 0.45\|3021\rangle$

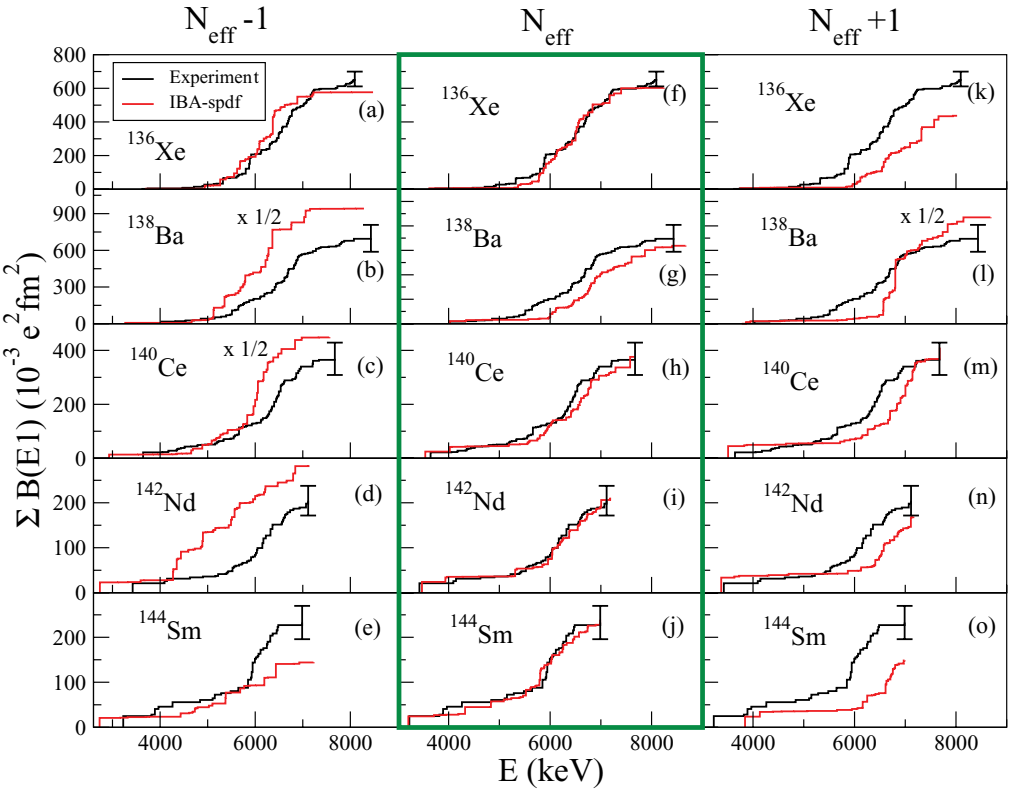

FIG. 4. (Color online) Comparison between the experimental and calculated integrated $E1$ strength for the stable even-even $N = 82$ isotones. The calculations are performed for three choices of the effective boson number: $N_{\rm eff}-1$ [(a)–(e)], $N_{\rm eff}$ [(f)–(j), also marked with a heavy-black (green) box], and $N_{\rm eff}+1$ [(k)–(o)]. The calculated sum is taken up to the energy at which the experimental information ends. A small shift in energy between experiment and calculated running sums can be observed in ^{138}Ba; but in each case, the final value agrees very well with the measured value, within the experimental uncertainties [marked only for the total $B(E1)$ strengths].

In Table I the strongest components of basis states of the wave functions for the first 1^- states in each analyzed nucleus are displayed. For illustrative purposes, the representations of the basis states have been simplified and are given in terms of bosons of a specific type: $|[n_s][n_p][n_d][n_f]\rangle$. Only the contributions with an amplitude higher than 10% are included. From the calculations one can see that the wave function of the first 1^- state in all stable $N = 82$ even-even nuclei is dominated by the coupling of d and f bosons, with almost no contribution from the p boson. This is in good agreement with the previous theoretical studies which identified the first 1^- state in these nuclei with the two-phonon state (corresponding to a coupling of the first 2^+ excitation with the first 3^- state).

The good reproduction of the experimentally observed $E1$ strength by the IBA-$spdf$ calculations can be observed in Fig. 4, where the results for the integrated $E1$ strength ("running sum") are presented for the stable $N = 82$ isotones. The calculations are performed for three choices of the effective boson number: $N_{\rm eff}-1$ [panels (a)–(e)], $N_{\rm eff}$ [(f)–(j)], and $N_{\rm eff}+1$ [(k)–(o)], where $N_{\rm eff}$ is the effective boson number given in Fig. 1. The calculated sum is taken up to the energy at which the experimental information ends. For the calculations using the effective boson number from Fig. 1, a small shift (around 300 keV) between experiment and calculated running sum can be observed in ^{138}Ba. For all the other nuclei the shift has a vanishing small value, pointing to a very good description of the distribution and fragmentation of the $E1$ strength. Also, the decrease of total strength from ^{136}Xe to ^{144}Sm observed experimentally is nicely reproduced by the IBA calculations. In each case the final values of the summed strength agrees very well with the measured values, within the experimental uncertainties. For the other effective boson number choices ($N_{\rm eff}-1$ and $N_{\rm eff}+1$), the integrated $E1$ strength is usually under predicted or has a different distribution pattern with increasing excitation energy. The calculations are performed using the same parameters given in Fig. 2. The distribution of the 1^- states can be improved to some degree by adjusting the a_3 and a_4 parameters in the Hamiltonian, but the $E1$ strength distribution on individual states is not severely affected by this choice. As seen in Fig. 4, the integrated $E1$ strength can be reproduced only by a specific set of boson numbers.

To further investigate the good reproduction of the $E1$ strength distribution, it is interesting to look also at the separate contribution to the integrated $E1$ strength of the three different terms in Eq. (3). The squared contributions of each term are plotted in Fig. 5 [both the $B(E1)$ distribution and the 'running sum'] for ^{142}Nd, where the agreement between the experimental and calculated $E1$ strength is the best (see Fig. 4). One can see that in the low-energy part of the distribution the higher contribution comes from the coupling of d and f bosons, while in the higher energy part (above 6 MeV), there is a competition between the d-f and p-d terms, the last one dominating the final part of the spectrum. This means that at higher excitation energies the p boson starts to play an important role in producing the $E1$ strength. This can be better understood if one considers the dipole and octupole

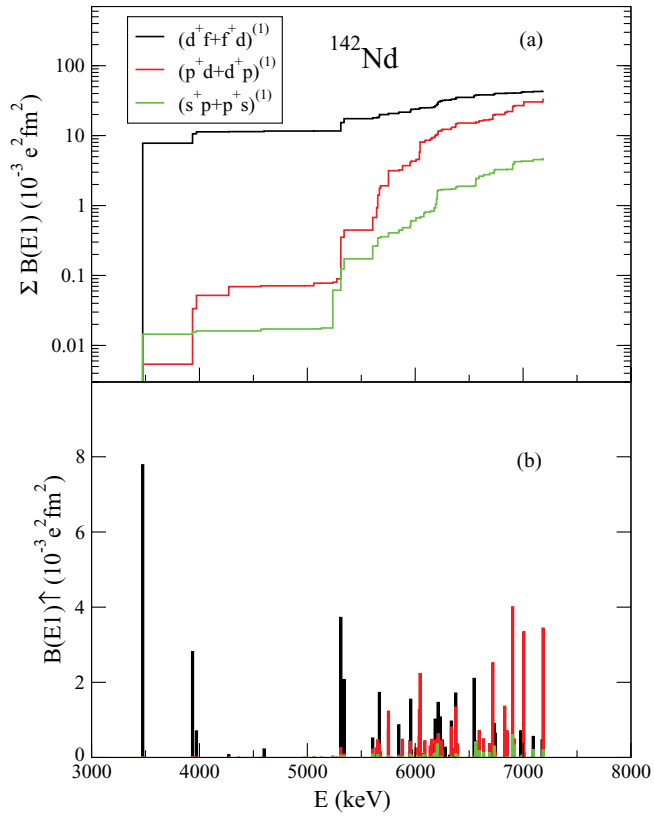

FIG. 5. (Color online) Comparison between the separate contribution to the (a) integrated and (b) absolute $E1$ strength distribution of the three different terms in Eq. (3). While in the low-energy part of the distribution the higher contribution comes from the coupling of d and f bosons, in the higher energy part, the p bosons start to play an important role in producing the $E1$ strength.

deformation of these states. These quantities are defined as

$$\text{Dipole deformation} = \frac{\langle \hat{n}_p \rangle}{\langle \hat{n}_d \rangle}, \tag{4}$$

and

$$\text{Octupole deformation} = \frac{\langle \hat{n}_f \rangle}{\langle \hat{n}_d \rangle}, \tag{5}$$

where $\langle \hat{n}_p \rangle$, $\langle \hat{n}_f \rangle$, and $\langle \hat{n}_d \rangle$ are the p, f, and d content of each state, respectively. In the low-energy part of the spectrum (up to around 6 MeV) the octupole deformation is dominant (roughly 25%) while the dipole deformation accounts only for about 2%. In the high-energy part, the situation is reversed and the dipole deformation gives rise to an enhanced $E1$ strength. The crossing point is again situated around 6 MeV, where the p-d term becomes dominant.

Another test for the IBA calculations is the distribution of states and the fragmentation of the $B(E1)$ strength. For this purpose the procedure given in Ref. [7] was followed. We begin the discussion with distribution of states in stable even-even $N = 82$ isotones. To focus on the distribution, the states are grouped in 250-keV-wide energy bins. The comparison between the experimental distribution and the calculated one is given in Fig. 6 for the effective boson numbers from Fig. 1. By using $N_{\rm eff}$, the IBA-$spdf$ calculations give a larger number

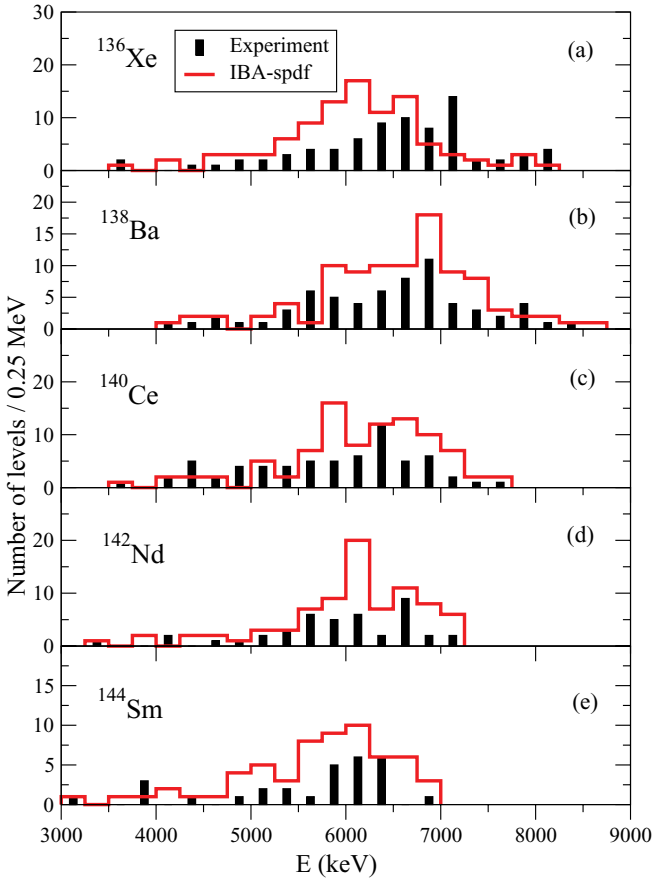

FIG. 6. (Color online) Comparison between the experimental and calculated distribution of states for the stable even-even $N = 82$ isotones. The states are grouped in energy bins 250-keV wide and the number of states for each bin is counted. A resonance-like structure is clearly observed both experimentally and theoretically between 5 and 8 MeV (see the text for details).

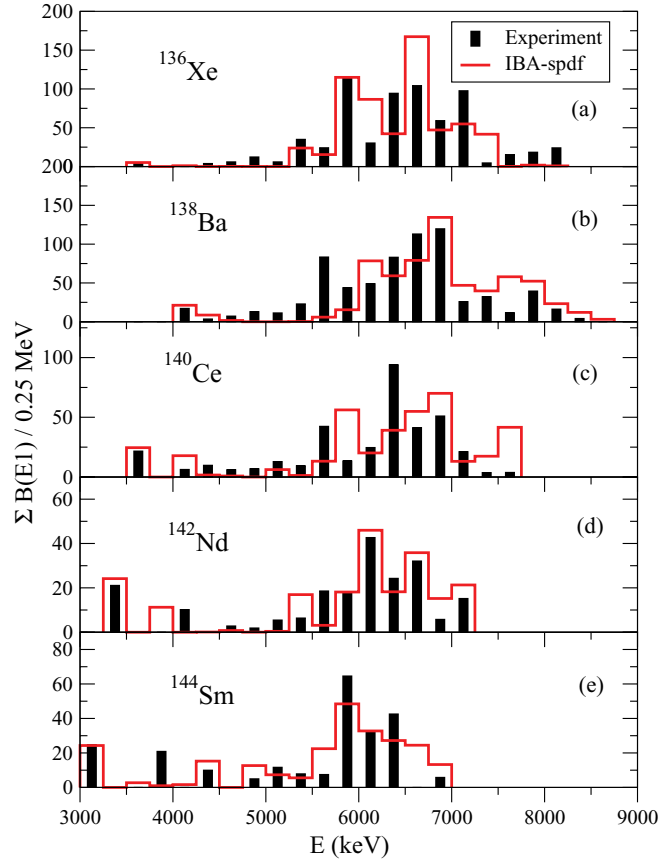

FIG. 7. (Color online) Comparison between the experimental and calculated distribution of $E1$ strength for the stable even-even $N = 82$ isotones. The states are grouped in energy bins 250-keV wide and the integrated $E1$ strength for each bin is counted (see the text for more details).

of states than the corresponding amount of levels observed experimentally by a factor that does not exceed 2 in any nucleus. Most of the states produced in excess are lying in the resonance-like region between 5 and 7 MeV, but do not carry much strength. This is in a rather good agreement with the results given by the quasiparticle-phonon model (QPM) calculations presented in Ref. [7], which predict a number of additional excited configurations when taking into account three particle-hole components. Similar to our calculations, many of these states produced by the QPM do not carry much strength [7].

A comparison between the experiment and the calculated values for the distribution of the $E1$ strength is presented in Fig. 7 as a function of the energy binning. The integrated $B(E1)$ strength is calculated for each bin. There is a remarkable agreement between the experiments and the IBA calculations for the summed $B(E1)$ values for most of the energy bins. Again, our results agree with the QPM calculations presented in Ref. [7]. This agreement indicates that the distribution of both states and $E1$ strength of the PDR can be reproduced by a simple phenomenological model like the IBA.

To further investigate the PDR properties, one has to look also at the fragmentation of the observed PDR states. A comparison between the experimental and calculated fragmentation is given in Fig. 8. Here, the states are grouped in $1 \times 10^{-3}\ e^2\,\mathrm{fm}^2$ wide bins and the number of levels for each bin is counted. It can be seen that for the low-strength excitations, the calculations exceed the experimental values. The same situation is encountered for the QPM calculations in Ref. [7]. However, in IBA, these excitations do not carry too much strength and the effect of these states on the integrated total strength is negligible.

To finalize the study for the fragmentation of the PDR properties we have to investigate also the fragmentation of the $B(E1)$ strength distribution. A comparison between experimental data and theoretical calculations is presented in Fig. 9. Again, the states are grouped in $1 \times 10^{-3}\ e^2\,\mathrm{fm}^2$ wide bins and the summed $E1$ strength is calculated for each bin. In this way, one can look at how the strength is distributed over the individual states. A good agreement between experimental data and theoretical calculations could be concluded. The main difference arises here between the IBA and QPM descriptions of the low-strength excitations [$B(E1) \leqslant 2 \times 10^{-3}\ e^2\,\mathrm{fm}^2$]. This is the region of the experimental limit, defined by the authors of Ref. [11] as being the minimum strength

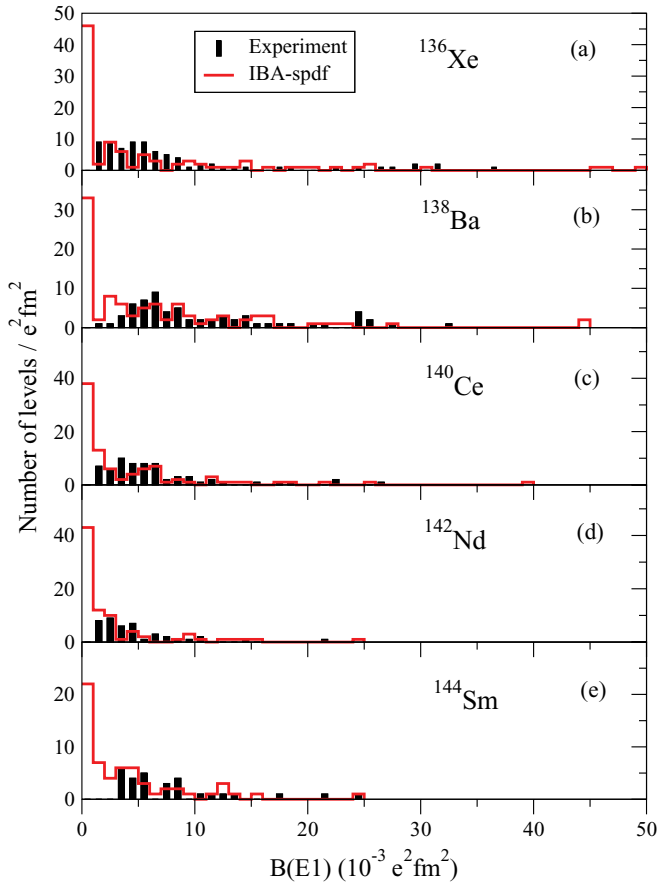

FIG. 8. (Color online) Comparison between the experimental and calculated fragmentation of PDR states for the stable even-even $N = 82$ isotones. The states are grouped in bins $1 \times 10^{-3}\ e^2\,\mathrm{fm}^2$ wide and the number of levels for each bin is presented (see the text for more details).

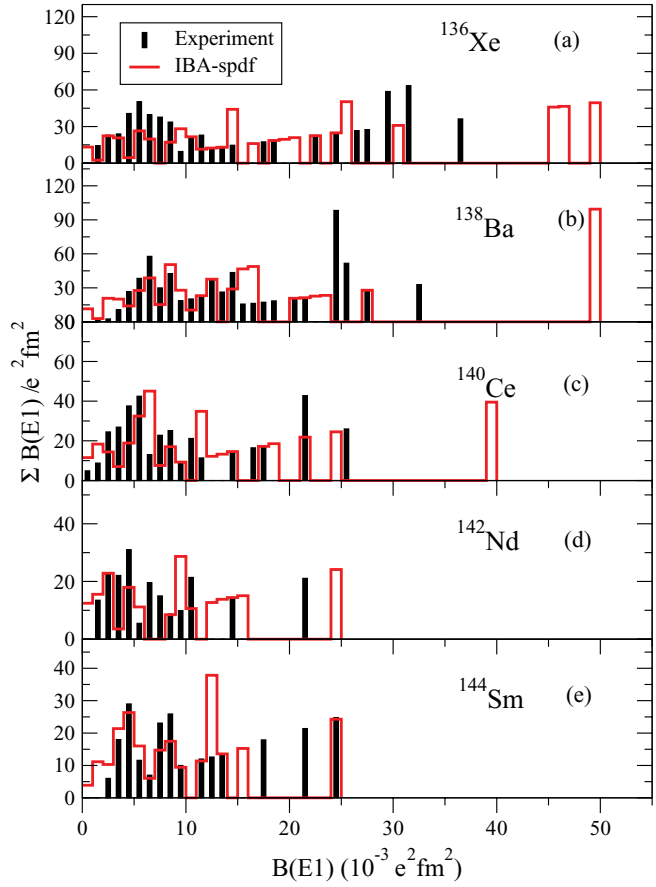

FIG. 9. (Color online) Analysis of the fragmentation of the $E1$ strength in the experimentally observed distribution and within the IBA model for the stable even-even $N = 82$ isotones (see the text for more details).

for an excitation to result in a peak above the background observed in the spectrum. In this region IBA predicts a similar $B(E1)$ strength as for the $B(E1) \simeq 2 \times 10^{-3}\ e^2\,\mathrm{fm}^2$ region (around 10–20 $\times\ 10^{-3}\ e^2\,\mathrm{fm}^2$). The QPM calculations [11] predict that the experiment misses strength in this region [the integrated strength for the $B(E1) \leqslant 2 \times 10^{-3}\ e^2\,\mathrm{fm}^2$ region is $\simeq 200 \times 10^{-3}\ e^2\,\mathrm{fm}^2$ for each nucleus]. Therefore, by taking into account this experimental limit in the QPM calculations, the agreement between theory and experiment is clearly improved. By applying the same experimental limit to the IBA calculations presented in Figs. 4–9 [integrated $B(E1)$ strength, distribution, and fragmentation], the main characteristics of the PDR remain practically unchanged. It is possible that for this small region the QPM calculations would yield a better result than the present IBA predictions. A comparison with some very sensitive experimental data that can lower the detection limit well below $B(E1) = 2 \times 10^{-3}\ e^2\,\mathrm{fm}^2$ is clearly needed.

The detailed comparison between the experimental results and IBA-$spdf$ calculations for stable even-even $N = 82$ isotones revealed that the main characteristics of the PDR can be reproduced by the IBA model. The calculations confirmed a good agreement for the distribution and fragmentation of the $E1$ strength.

V. IBA PREDICTIONS OF THE PYGMY DIPOLE RESONANCE IN ^{94}Mo

In the previous section it was shown that IBA can account for most of the observed properties of the PDR in stable even-even $N = 82$ isotones. From a theoretical point of view it is interesting to see if the procedure employed in this paper can be used to describe the PDR properties in other regions of the nuclear chart. To perform such an investigation we chose the $N = 52$ region, and we concentrate in this section on the study of ^{94}Mo.

For the present calculations we used the same extended basis for diagonalization allowing up to three negative parity bosons. The experimental data for the low-lying states are taken from Ref. [51]. The experimental information concerning the energies of the 1^- states is taken from Ref. [52] and is used to fit the parameters of the Hamiltonian in Eq. (1). However, because of some inconsistencies that were found in this experiment, we cannot trust the absolute values of the $B(E1)$ strength. These quantities are the ones that we want to predict, and not the energies of the individual states.

From a boson counting perspective, the structure of ^{94}Mo should be similar to the one of ^{136}Xe (two bosons counted in a traditional way). This is the reason why we adopted the same number of effective bosons for the IBA calculations of both

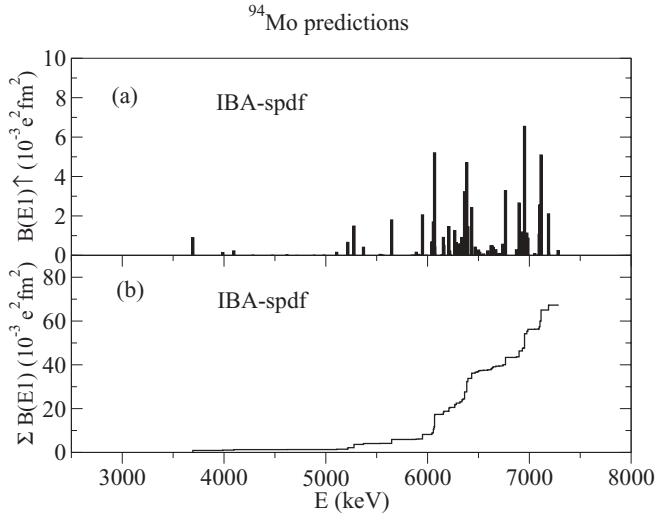

FIG. 10. IBA-$spdf$ predictions for the PDR properties of ^{94}Mo. (a) Individual $E1$ strengths of the PDR states. (b) Total summed strength predicted by the calculations.

^{136}Xe and ^{94}Mo, $N_{\rm eff} = 6$. The parameters of the Hamiltonian from Eq. (1) were chosen such that they reproduce the low-lying states of this nucleus: $\epsilon_d = 0.871$ MeV, $\epsilon_f = 2.534$ MeV (the energy values of the first 2^+ and 3^- states, respectively), $a_3 = 0.40$ MeV, and $a_4 = 0.57$ MeV (identical to the ones in ^{136}Xe). The quadrupole deformation parameter was kept at a similar value as for the stable even-even $N = 82$ isotones ($\kappa = -0.025$ MeV). The p-boson energy is fixed at the typical value for the $N = 82$ isotones ($\epsilon_p = 6.0$ MeV). Because of the lack of detailed experimental results [53], there were not sufficient data to constrain the $E1$ operator parameters. However, to have an estimation of the $E1$ strengths, we adopted the following procedure. The $E1$ operator parameters employed were the same as for ^{136}Xe: $e_1 = 0.17\ e\ \mathrm{b}^{1/2}$, $\chi_{sp} = 0.63$, and $\chi_{df} = 0.24$. The $B(E1)$ value of the first 1^- state can be derived from the lifetime of this state measured in Ref. [54] and has a value of $\simeq 0.9 \times 10^{-3}\ e^2\,\mathrm{fm}^2$. The obtained $B(E1)$ strengths for all the 1^- states produced by the IBA model were normalized to this value.

The predictions of the IBA-$spdf$ calculations for the PDR properties of ^{94}Mo are given in Fig. 10. In panel (a) the individual $E1$ strength of the PDR states are given. Between 5 and 7 MeV a resonance-like structure is predicted by the IBA calculations, pointing to a similar behavior as for the stable even-even $N = 82$ isotones. In panel (b) the integrated $E1$ strength predicted by the calculations is presented. The summed $E1$ strength is predicted to have a value of $0.070\ e^2\,\mathrm{fm}^2$. Remarkably, this value is roughly 10 times lower than the corresponding value in ^{136}Xe, although the parameters used in the $E1$ calculations were the same. Clearly the measurement of these data will finally establish if the picture predicted by the IBA model is correct. Additional calculations performed within a modern microscopic model (QPM, QRPA) will clarify whether this effect can be connected with the oscillation of the neutron skin against the isospin saturated core.

VI. CONCLUSIONS

The pygmy dipole resonance in stable even-even $N = 82$ isotones was investigated in the framework of the IBA-$spdf$ model with effective boson numbers. A detailed comparison between the experimental results and the IBA calculations has been performed for all stable even-even $N = 82$ isotones. The calculations predict a resonance-like structure between 5 and 8 MeV, very similar to the experimental results and to other theoretical calculations performed within the QPM. The calculations confirm a good agreement for the distribution and fragmentation of the $E1$ strength. This represents a strong argument in favor of the collective nature of the PDR. In the last section, the predictions of the PDR strength for ^{94}Mo are given. The measurement of these data will establish if the picture predicted by the IBA model is correct. In addition, microscopic calculations are needed to establish the connection between the experimental observed states and the assumption of an out-of-phase oscillation of the neutron skin against the isospin saturated core.

ACKNOWLEDGMENTS

The authors thank P. von Brentano and D. Savran for stimulating discussions. This work was supported by the Deutsche Forschungsgemeinschaft under Contract No. ZI 510/4-1.

[1] M. N. Harakeh and A. van der Woude, *Giant Resonances* (Oxford University, Oxford, 2001).
[2] G. A. Bartholomew, E. D. Earle, A. J. Ferguson, J. W. Knowles, and M. A. Lone, Adv. Nucl. Phys. **7**, 229 (1973).
[3] R.-D. Herzberg *et al.*, Phys. Rev. C **60**, 051307(R) (1999).
[4] A. Zilges, S. Volz, M. Babilon, T. Hartmann, P. Mohr, and K. Vogt, Phys. Lett. B **542**, 43 (2002).
[5] P. Adrich *et al.*, Phys. Rev. Lett. **95**, 132501 (2005).
[6] S. Volz, N. Tsoneva, M. Babilon, M. Elvers, J. Hasper, R.-D. Herzberg, H. Lenske, K. Lindenberg, D. Savran, and A. Zilges, Nucl. Phys. A **779**, 1 (2006).
[7] D. Savran, M. Fritzsche, J. Hasper, K. Lindenberg, S. Muller, V. Y. Ponomarev, K. Sonnabend, and A. Zilges, Phys. Rev. Lett. **100**, 232501 (2008).
[8] O. Wieland *et al.*, Phys. Rev. Lett. **102**, 092502 (2009).
[9] J. Endres *et al.*, Phys. Rev. Lett. **105**, 212503 (2010).
[10] A. P. Tonchev, S. L. Hammond, J. H. Kelley, E. Kwan, H. Lenske, G. Rusev, W. Tornow, and N. Tsoneva, Phys. Rev. Lett. **104**, 072501 (2010).
[11] D. Savran *et al.*, Phys. Rev. C **84**, 024326 (2011).
[12] D. Savran, M. Babilon, A. M. vanden Berg, M. N. Harakeh, J. Hasper, A. Matic, H. J. Wortche, and A. Zilges, Phys. Rev. Lett. **97**, 172502 (2006).
[13] R. Mohan, M. Danos, and L. C. Biedenharn, Phys. Rev. C **3**, 1740 (1971).
[14] J. Piekarewicz, Phys. Rev. C **73**, 044325 (2006).
[15] T. Aumann, Eur. Phys. J. A **26**, 441 (2005).
[16] D. L. Lambert, Astron. Astrophys. Rev. **3**, 201 (1992).

[17] S. Goriely, E. Kahn, and M. Samyn, Nucl. Phys. A **739**, 331 (2004).
[18] C. J. Horowitz and J. Piekarewicz, Phys. Rev. Lett. **86**, 5647 (2001).
[19] A. W. Steiner, M. Prakash, J. M. Lattimer, and P. J. Ellis, Phys. Rep. **411**, 325 (2005).
[20] A. Klimkiewicz *et al.*, Nucl. Phys. A **788**, 145 (2007).
[21] Y. Suzuki, K. Ikeda, and H. Sato, Prog. Theor. Phys. **83**, 180 (1990).
[22] P. Van Isacker, M. A. Nagarajan, and D. D. Warner, Phys. Rev. C **45**, R13 (1992).
[23] J. Chambers, E. Zaremba, J. P. Adams, and B. Castel, Phys. Rev. C **50**, R2671 (1994).
[24] G. Colò, N. Van Giai, P. F. Bortignon, and M. R. Quaglia, Phys. Lett. B **485**, 362 (2000).
[25] N. Paar, D. Vretenar, E. Khan, and G. Colò, Rep. Prog. Phys. **70**, 691 (2007).
[26] N. Tsoneva, H. Lenske, and Ch. Stoyanov, Phys. Lett. B **586**, 213 (2004).
[27] N. Tsoneva and H. Lenske, Phys. Rev. C **77**, 024321 (2008).
[28] E. Litvinova, P. Ring, and V. Tselyaev, Phys. Rev. C **78**, 014312 (2008).
[29] T. Hartmann, M. Babilon, S. Kamerdzhiev, E. Litvinova, D. Savran, S. Volz, and A. Zilges, Phys. Rev. Lett. **93**, 192501 (2004).
[30] V. Tselyaev, J. Speth, F. Grümmer, S. Krewald, A. Avdeenkov, E. Litvinova, and G. Tertychny, Phys. Rev. C **75**, 014315 (2007).
[31] G. Tertychny, V. Tselyaev, S. Kamerdzhiev, F. Grümmer, S. Krewald, J. Speth, A. Avdeenkov, and E. Litvinova, Phys. Lett. B **647**, 104 (2007).
[32] M. Sambatoro and G. Molnar, Nucl. Phys. A **376**, 201 (1982).
[33] M. Sambatoro, Nucl. Phys. A **380**, 365 (1982).
[34] K. Heyde, P. Van Isacker, M. Waroquier, G. Wenes, and M. Sambataro, Phys. Rev. C **25**, 3160 (1982).
[35] P. D. Duval and B. R. Barrett, Phys. Lett. B **100**, 223 (1981).
[36] G. Cata, D. Bucurescu, D. Cutoiu, M. Ivaşcu, and N. V. Zamfir, Zeitschrift für Physik A Hadrons and Nuclei, Atomic Nuclei **335**, 271 (1990).
[37] R. F. Casten and D. D. Warner, Rev. Mod. Phys. **C 60**, 389 (1988).
[38] N. V. Zamfir and D. Kusnezov, Phys. Rev. C **63**, 054306 (2001).
[39] D. Kusnezov, J. Phys. A **22**, 4271 (1989).
[40] M. Ogawa, R. Broda, K. Zell, P. J. Daly, and P. Kleinheinz, Phys. Rev. Lett. **41**, 289 (1978).
[41] O. Scholten, Phys. Lett. B **127**, 144 (1983).
[42] H. T. Hsieh, H. C. Chiang, M. M. King Yen, and D. S. Chuu, J. Phys. G **12**, 167 (1986).
[43] D. Kusnezov, computer code OCTUPOLE (unpublished).
[44] A. A. Sonzogni, Nucl. Data Sheets **95**, 837 (2002).
[45] A. A. Sonzogni, Nucl. Data Sheets **98**, 515 (2003).
[46] N. Nica, Nucl. Data Sheets **108**, 1287 (2007).
[47] T. D. Johnson, D. Symochko, M. Fadil, and J. K. Tuli, Nucl. Data Sheets **112**, 1949 (2011).
[48] A. A. Sonzogni, Nucl. Data Sheets **93**, 599 (2001).
[49] M. Babilon, N. V. Zamfir, D. Kusnezov, E. A. McCutchan, and A. Zilges, Phys. Rev. C **72**, 064302 (2005).
[50] J. Engel and F. Iachello, Nucl. Phys. A **472**, 61 (1987).
[51] D. Abriola and A. A. Sonzogni, Nucl. Data Sheets **107**, 2423 (2006).
[52] C. Romig (private communication).
[53] M. Erhard, A. R. Junghans, C. Nair, R. Schwengner, R. Beyer, J. Klug, K. Kosev, A. Wagner, and E. Grosse, Phys. Rev. C **81**, 034319 (2010).
[54] C. Fransen *et al.*, Phys. Rev. C **67**, 024307 (2003).